Monthly Notices
of the
ROYAL ASTRONOMICAL SOCIETY

MNRAS **430,** 2768–2773 (2013) doi:10.1093/mnras/stt077

Obscured star formation in Lyα blobs at $z = 3.1$

Y. Tamura,[1]⋆ Y. Matsuda,[2,3] S. Ikarashi,[1] K. S. Scott,[4] B. Hatsukade,[5] H. Umehata,[1] T. Saito,[6] K. Nakanishi,[3,7,8] M. S. Yun,[9] H. Ezawa,[3] D. H. Hughes,[10] D. Iono,[3,11] R. Kawabe,[3,7] K. Kohno[1] and G. W. Wilson[9]

[1]*Institute of Astronomy, The University of Tokyo, Mitaka, Tokyo 181-0015, Japan*
[2]*California Institute of Technology, MC 105-24, 1200 East California Boulevard, Pasadena, CA 91125, USA*
[3]*National Astronomical Observatory of Japan, Mitaka, Tokyo 181-8588, Japan*
[4]*North American ALMA Science Center, National Radio Astronomy Observatory, Charlottesville, VA 22903, USA*
[5]*Department of Astronomy, Kyoto University, Kyoto 606-8502, Japan*
[6]*Kavli Institute for the Physics and Mathematics of the Universe, The University of Tokyo, Kashiwanoha, Kashiwa 277-8583, Japan*
[7]*Joint ALMA Observatory, Alonso de Cordova 3107, Vitacura, Santiago 763 0355, Chile*
[8]*The Graduate University for Advanced Studies (Sokendai), Mitaka, Tokyo 181-8588, Japan*
[9]*Department of Astronomy, University of Massachusetts, Amherst, MA 01003, USA*
[10]*Instituto Nacional de Astrofísica, Óptica y Electrónica (INAOE), Apartado Postal 51 y 216, 72000 Puebla, Pue., Mexico*
[11]*Nobeyama Radio Observatory, National Astronomical Observatory of Japan, Minaminaki, Minamisaku, Nagano 384-1305, Japan*

Accepted 2013 January 11. Received 2013 January 9; in original form 2012 May 30

ABSTRACT

We present results from the AzTEC/ASTE 1.1-mm imaging survey of 35 Lyα blobs (LABs) found in the SSA22 protocluster at $z = 3.1$. These 1.1-mm data reach an rms noise level of 0.7–1 mJy beam^{-1}, making this the largest millimetre-wave survey of LABs to date. While one (or possibly two) out of 35 LABs might be detected at 3σ level, no significant ($\geq 3.5\sigma$) emission is found in any of individual 35 LABs. From this, we estimate 3σ upper limits on the far-infrared luminosity of $L_{\rm FIR} < 2 \times 10^{12}$ L$_\odot$ (the dust temperature of 35 K and the emissivity index of 1.5 are assumed). Stacking analysis reveals that the 1.1-mm flux density averaged over the LABs is $S_{1.1\,\rm mm} < 0.40$ mJy (3σ), which places a constraint of $L_{\rm FIR} < 4.5 \times 10^{11}$ L$_\odot$. These data constrain the dust spectral energy distributions of the LABs more tightly than ever if their spectral indices at rest-frame wavelength of ≈ 240 μm are similar to those found in (ultra-)luminous infrared galaxies at $0.2 < z < 0.3$. Our results suggest that LABs on average have little ultraluminous obscured star formation, in contrast to a long-believed picture that LABs undergo an intense episode of dusty star formation activities with star formation rates of $\sim 10^3$ M$_\odot$ yr^{-1}. Observations with the Atacama Large Millimeter/submillimeter Array are needed to directly study the obscured part of star formation activity in the LABs.

Key words: galaxies: evolution – galaxies: formation – galaxies: high-redshift – galaxies: starburst.

1 INTRODUCTION

Lyα blobs (LABs) are characterized by extended (20–300 kpc) Lyα nebulae that are often found in overdense regions at high redshift. The origin of Lyα nebulosity, however, is mysterious. There are possible explanations for the origin: the scenario that was first proposed is that the Lyα nebulae are produced by mechanical feedback (or 'superwind') or photoionization from active galactic nuclei (AGN) and/or massive star formation activities (Taniguchi & Shioya 2000; Taniguchi, Shioya & Kakazu 2001; Ohyama et al. 2003; Mori & Umemura 2006). In fact, ultraviolet (UV) continuum and/or 24-μm emission, the latter arising from starburst/AGN heating of dust, are often detected in LABs (Steidel et al. 2000; Matsuda et al. 2004), which can provide the sufficient number of ionizing photons (Geach et al. 2009; Webb et al. 2009; Colbert et al. 2011) to account for the Lyα luminosities ($L_{\rm Ly\alpha} \gtrsim 10^{42.5}$ erg s^{-1}, e.g. Matsuda et al. 2004, 2011; Saito et al. 2006, 2008). The large velocity width of the Lyα emission ($\sim$550 km s^{-1}; Matsuda et al. 2006) can also be accounted for by the superwind scenario. On the other hand, a sizeable number of LABs which lack evidence of such apparent heating sources have been reported. This fact imposes an alternative scenario in which the origin of Lyα nebulae is attributed to cooling radiation from primeval hydrogen gas which accretes on to massive

⋆E-mail: ytamura@ioa.s.u-tokyo.ac.jp

dark haloes (aka cold accretion; e.g. Fardal et al. 2001; Nilsson et al. 2006; Smith et al. 2008), although there remains the possibility that the ionizing sources are hidden by the interstellar medium located along the line of sight.

Observations of obscured star formation and/or AGN are therefore necessary to properly understand the origins of the Lyα nebulosity. Many attempts to detect the interstellar cold dust and molecular gas in LABs at millimetre (mm) and sub-mm wavelengths have been carried out (Chapman et al. 2001, 2004; Geach et al. 2005; Matsuda et al. 2007; Beelen et al. 2008; Yang et al. 2012). However, whether LABs have intense star formation activities that are capable of producing and maintaining the Lyα haloes is still controversial.

In this paper, we present the results from our unbiased 1.1-mm survey of 35 LABs at $z = 3.1$ found in optical narrow-band filter observations (Steidel et al. 2000; Matsuda et al. 2004) towards the SSA22 field, which is known for having an overdensity of Lyα emitters (LAEs) at $z = 3.09$ (Hayashino et al. 2004). This is the largest mm survey of LABs to date, for which we can study the obscured star formation of these systems. The structure of this paper is as follows. In Section 2, we describe our 1.1-mm observations and data reduction. Section 3 describes the results. Finally, we have brief discussions and a summary in Section 4. Throughout this paper, we assume a concordance cosmology with $\Omega_{\rm m} = 0.3$, $\Omega_\Lambda = 0.7$, $H_0 = 70$ km s^{-1} Mpc^{-1}, where 1 arcsec corresponds to a physical scale of 7.64 kpc at $z = 3.09$.

2 OBSERVATIONS

The data were taken with the AzTEC 1.1-mm camera (Wilson et al. 2008) installed on the Atacama Submillimeter Telescope Experiment (ASTE; Ezawa et al. 2004) located at Pampa la Bola, Atacama desert, Chile. The data taken during 2007 July–September are described in Tamura et al. (2009). In addition to the 2007 data, we added new data taken in 2008 that almost triple the survey area to 0.27 deg^2. The complete description will be given elsewhere (Umehata et al., in preparation).

The reduction procedure is described in Scott et al. (2008) and Downes et al. (2012). The time-stream data were intensively cleaned using a principal component analysis (PCA) algorithm, and then mapped. The full width at half-maximum of the point response function is 34 arcsec, corresponding to 260 kpc in physical scale at $z = 3.1$. The pointing was checked every 1 hr. Uranus and Neptune were used for flux calibration, yielding an absolute accuracy better than 10 per cent. The resulting rms noise over the region covering 0.27 deg^2 is 0.7–1.2 mJy beam^{-1} ($\leq$0.8 mJy beam^{-1} for 30 out of the 35 LABs). Note that stacking analysis for *Spitzer*/MIPS, IRAC and Very Large Array (VLA) sources in SSA22 shows no systematic error in astrometry down to better than 4 arcsec. Submillimeter Array (SMA) 860-μm imaging of the brightest 1.1-mm source, SSA22-AzTEC1 (Tamura et al. 2010), also supports this.

3 RESULTS

In this section, we first discuss tentative detections of 1.1-mm emission from individual LABs in Section 3.1. We then consider a statistical detection of the average 1.1-mm properties of the LABs in Section 3.2.

3.1 1.1-mm emission of individual LABs

We do not find significant ($\geq 3.5\sigma$) 1.1-mm emission for any of the 35 LABs, as shown in Fig. 1 and Table 1, which lists the 1.1-mm flux density measured at the locations of the LABs. Although the peak of Lyα emission may not always coincide with the 1.1-mm counterpart, the offset can be negligible because the Lyα extent is well within the beam (34 arcsec). If we assume a dust temperature of $T_{\rm dust} = 35$ K and a dust emissivity index of $\beta = 1.5$, the 3σ upper limit places a constraint on far-infrared (FIR) luminosity of $L_{\rm FIR} < 2 \times 10^{12}\,{\rm L}_\odot$ for the LABs. This limit corresponds to a star formation rate (SFR) of $\approx$400 M$_\odot$ yr^{-1}, which suggests that LABs do not have intense dust-obscured star formation activity found in sub-mm galaxies (SMGs; Blain et al. 2002, for a review). Given that our 1.1-mm map reveals >100 SMGs over the SSA22 region (Tamura et al., in preparation), none of which coincide with the LABs, this result strongly suggests that the LAB population is essentially different from the SMG population.

We note that SPIRE/*Herschel* data that have recently been taken towards SSA22 (PI: Matsuda) are in good agreement with the 1.1-mm results. The 35 LABs have no SPIRE 500-μm counterpart. While low-S/N 250-μm enhancements are seen at the positions of a few LABs, the flux densities rapidly dim towards longer wavelengths, implying that the dust emission seen at 250 μm is due to high dust temperatures and/or low-z contaminants. However, identification of exact 250-μm counterparts is beyond the scope of this paper.

In the rest of this section, we discuss three tentative ($>2\sigma$) detections of the 1.1-mm emission from three of the LABs.

SSA22-LAB1: LAB1 was originally discovered by an optical narrow-band filter survey towards SSA22 (Steidel et al. 2000), and is one of the most-studied LABs in the mm and sub-mm. Subsequent imaging and photometric observations with the Submillimetre Common-User Bolometer Array (SCUBA; Holland et al. 1999) on the James Clerk Maxwell Telescope had revealed a luminous 850-μm source at the position of LAB1 with $S_{850\,\mu{\rm m}} = 16.8 \pm 2.9$ mJy (Chapman et al. 2001, 2004). However, the SMA 880-μm imaging found no emission, suggesting that the spatial extent of the sub-mm emission of LAB1 should be larger than 4 arcsec (Matsuda et al. 2007). Very recently, Yang et al. (2012) have reported a non-detection of mm and sub-mm emission, suggesting that there is no dusty starburst associated with the LAB as reported by Chapman et al. (2001, 2004). Our new 1.1-mm map shows only a marginal enhancement of 1.9 mJy beam^{-1} (2.7σ) relative to the noise. These low-resolution, single-dish observations cast doubt on the presence of an extended dust component that could account for the SMA non-detection.

Furthermore, the 850-to-1100-μm flux ratio would be >8, which is quite high compared with a typical starburst galaxies. The 850–1100 μm band corresponds to the rest-frame wavelengths of 210–270 μm for a $z = 3.1$ object. So, the 1.1-mm 3σ upper limit of 2.2 mJy places a constraint on the rest-frame spectral index at $\lambda_{\rm rest} = 240\,\mu$m[1] to $\alpha_{240\,\mu{\rm m}} = 7.85$ or higher. In Fig. 2, we show a histogram of $\alpha_{240\,\mu{\rm m}}$ measured in 70 (ultra)luminous infrared galaxies (U/LIRGs) with spectroscopic redshifts of $z = 0.2$–0.3. The U/LIRGs are catalogued in the *Herschel*-ATLAS Science Demonstration Phase (SDP; Eales et al. 2010; Pascale et al. 2011; Rigby et al. 2011; Smith et al. 2011) data base,[2] and all detected at 250 and 350 μm at $>5\sigma$. For $z = 0.2$–0.3 objects, the SPIRE 250–350 μm bands sample the rest-frame $\approx$240$-\mu$m part of the spectral energy distributions (SEDs). The mean H-ATLAS spectral index inferred from the 250-to-350-μm flux ratios is $\alpha_{240\,\mu{\rm m}} = 0.93 \pm 0.82$ (the

[1] This defines the slope of a spectrum such that $S_\nu \propto \nu^{\alpha_{240\,\mu{\rm m}}}$.
[2] www.h-atlas.org/public-data/

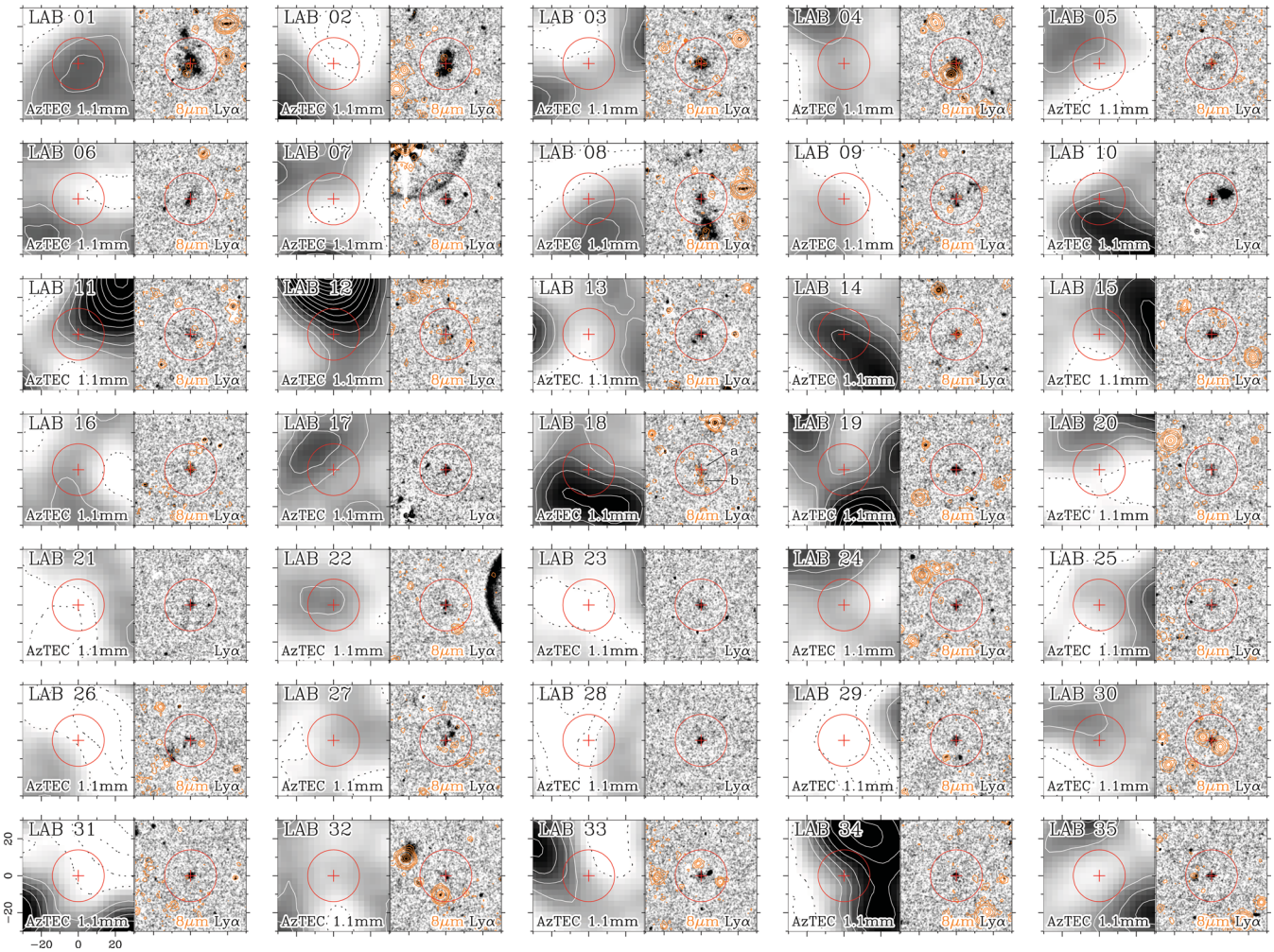

Figure 1. The left-hand panel: the 1.1-mm postage stamp images (60 arcsec × 60 arcsec) for all 35 LABs. The contours start from 1σ with an interval of 1σ. The negative signals are indicated by dotted contours. The 1σ noise levels are 0.7–1 mJy beam^{-1}, depending on locations across the 1.1-mm image. The right-hand panel: the Subaru NB497 − BV images, which indicate the intensity of Lyα emission at $z = 3.1$. The orange contours show IRAC 8 μm (Webb et al. 2009), which are drawn at (2, 5, 10, 20, 50, 100,...) times local noise levels ($1\sigma \approx 1 \times 10^{-2}$ MJy str^{-1} in typical).

error bar is from the standard deviation), which turns to be lower than expected in the Rayleigh–Jeans regime (this is simply because we are looking at the waveband close to the dust emission peak). The spectral index of LAB1 is extremely steep compared with the H-ATLAS indices, suggesting that the earlier SCUBA measurement remarkably overestimates the 850-μm flux density. On the other hand, our result is consistent with other recent non-detections with the SMA, LABOCA/APEX, and the Plateau de Bure Interferometer (Matsuda et al. 2007; Yang et al. 2012).

SSA22-LAB14: the 3.2σ enhancement is seen at the location of LAB14 (see Fig. 1), which is ≈25 arcsec north-eastwards from the SMG, SSA22-AzTEC69 (S/N = 4.1; Tamura et al., in preparation). The 1.1-mm flux density at the LAB14 position is 2.43 ± 0.76 mJy beam^{-1}, although heavy blending with SSA22-AzTEC69 makes it difficult to accurately measure the 1.1-mm flux density. Note that it is unlikely that SSA22-AzTEC69 is the mm counterpart to LAB14 since a Monte Carlo simulation (the method is given in Scott et al. 2008) shows a low probability ($p \lesssim 0.01$) that a S/N = 4 source is detected >20 arcsec away from its original position. LAB14 has been detected at 850 μm (SMM J221735.84+001558.9, $S_{850\,\mu m}$ = 4.9 ± 1.3 mJy; Chapman et al. 2005; Geach et al. 2005). The 850-to-1100-μm flux ratio would be 2.0 if assuming $S_{1.1\,mm} = 2.43 \pm 0.76$ mJy. This yields $\alpha_{240\,\mu m} = 2.72 \pm 2.53$, which is consistent with those found in the H-ATLAS galaxies (Fig. 2), although the 1.1-mm flux is tentative.

SSA22-LAB18: a SCUBA detection has been reported for this LAB ($S_{850\,\mu m} = 11.0 \pm 1.5$ mJy; Geach et al. 2005). It has two IRAC counterparts, LAB18-a and LAB18-b (Webb et al. 2009). The former coincides with the Lyα peak and has a 24-μm counterpart, whereas the latter has a hard X-ray source (Geach et al. 2009) but no 24-μm counterpart. We find an enhancement of 1.5 mJy (2.1σ) and 2.3 mJy (3.2σ) at the positions of LAB18-a and -b, respectively, but the two objects are likely blended by a nearby 1.1-mm source with S/N ≈ 4, located ≈20 arcsec south of LAB18-a (or ≈10 arcsec south of LAB18-b). The 850-to-1100-μm flux ratio of LAB18-a is >7.2 if taking the 3σ upper limit, while that of LAB18-b is 4.7 ± 1.6 if the flux density would be $S_{1.1\,mm} = 2.33 \pm 0.73$ mJy, although the source blending likely boosts the 1.1-mm flux density. The spectral indices at $\lambda_{rest} = 240$ μm are >7.7 and 6.0 ± 1.3 for LAB18-a and -b, respectively. Again, the $\alpha_{240\,\mu m}$ indices are substantially deviated from the H-ATLAS distribution (Fig. 2), implying that the SCUBA measurement might overestimate the 850-μm flux. Note that the

Table 1. The 1.1-mm properties of LABs in SSA22.

Name	1.1 mm results			Other results
	$S_{1.1\,\mathrm{mm}}$ (mJy)	σ (mJy)	S/N	$S_{850\,\mu\mathrm{m}}$ [a] (mJy)
LAB1[b]	1.97	0.74	2.7	**16.8 ± 2.9**
LAB2	−1.89	0.76	−2.4	3.3 ± 2.9
LAB3	−0.69	0.73	−0.9	−0.2 ± 1.2
LAB4	0.11	0.74	0.1	0.9 ± 1.5
LAB5	0.34	0.74	0.5	**5.2 ± 1.5**
LAB6	0.07	1.14	0.1	−0.5 ± 1.4
LAB7	−0.88	0.74	−1.2	0.2 ± 1.6
LAB8	0.67	0.74	0.9	0.3 ± 5.3
LAB9	0.07	0.74	0.1	1.3 ± 5.3
LAB10	1.20	0.84	1.4	**6.1 ± 1.4**
LAB11	0.61	0.73	0.8	−0.4 ± 5.3
LAB12	0.30	0.74	0.4	3.2 ± 1.6
LAB13	−0.72	0.73	−1.0	–
LAB14	2.43	0.76	3.2	**4.9 ± 1.3**
LAB15	−0.27	0.74	−0.4	–
LAB16	0.34	0.74	0.5	2.2 ± 5.3
LAB17	1.41	1.19	1.2	–
LAB18-a	1.53	0.73	2.1	**11.0 ± 1.5**
LAB18-b	2.33	0.73	3.2	
LAB19	−0.81	0.74	−1.1	−8.6 ± 5.3
LAB20	−0.80	0.75	−1.1	0.4 ± 1.5
LAB21	−1.37	0.75	−1.8	–
LAB22	1.04	0.74	1.4	–
LAB23	−1.55	0.80	−1.9	–
LAB24	0.03	0.72	0.0	–
LAB25	0.01	0.73	1.4	1.4 ± 5.3
LAB26	−0.90	0.74	−1.2	−2.7 ± 5.3
LAB27	0.18	0.77	0.2	0.5 ± 1.6
LAB28	−0.99	0.76	−1.3	–
LAB29	−2.54	0.91	−2.8	–
LAB30	0.65	0.74	0.9	3.3 ± 1.3
LAB31	−1.44	0.74	−1.9	−3.7 ± 5.3
LAB32	−0.16	0.74	−0.2	1.8 ± 1.4
LAB33	0.04	0.73	0.1	1.6 ± 1.5
LAB34	1.01	0.93	1.1	–
LAB35	−0.74	0.73	−1.0	1.2 ± 5.3
Mean	<0.40[c]	–	–	3.0 ± 0.9

[a]Observed by SCUBA (Chapman et al. 2001, 2004; Geach et al. 2005). The LABs detected at 850 μm with ≥3.5σ are indicated in boldface type.
[b]The 3σ upper limits of $S_{880\,\mu\mathrm{m}} < 4.2$ mJy (Matsuda et al. 2007), $S_{870\,\mu\mathrm{m}} < 12$ mJy and $S_{1.2\,\mathrm{mm}} < 0.45$ mJy (Yang et al. 2012) are reported.
[c] The 3σ upper limit.

southernmost 1.1-mm source is not likely to be the counterpart because the Monte Carlo simulation suggests a low probability ($p \lesssim 0.15$).

3.2 Stacking analysis

Stacking analysis, a pixel-to-pixel weighted-mean of two-dimensional images around objects of interest, is often used to statistically detect very faint emission features that are common among the objects. In order to measure the average 1.1-mm flux density of LABs, we stack the 1.1-mm images around the positions of (i) all of the LABs in SSA22, and (ii) the five SCUBA-detected LABs, for which Geach et al. (2005) have reported positive detections at 850 μm. Note that only LABs that are >30 arcsec away from any of mm-bright (≥3.5σ) point sources (Tamura et al., in preparation) are considered to eliminate the blending of the nearby bright sources; this leaves 32 (91 per cent) of the 35 LABs[3] and 3 of the 5 SCUBA-detected LABs.[4] The PCA cleaning process used in AzTEC reduction filters out low spatial frequency components of the map, resulting in axisymmetric negative sidelobes (≈− 7 per cent of the maximum) around a bright source. The sidelobes systematically offset the zero-point of a stacked image. In this analysis, we first deconvolved the 1.1-mm image with a point response function (details are given in Downes et al. 2012) using the CLEAN algorithm (Högbom 1974). The CLEAN-ed images that are cut out around the positions of the 32 LABs are weighted according to the local noise level, and then averaged. The 1σ noise level is estimated by calculating $(\sum_i \sigma_i^{-2})^{-1/2}$, where σ_i is the local rms noise level of the 1.1-mm image around the position of the ith LAB. We verify that the average (i.e. stacked) flux density of model sources is correctly reproduced by Monte Carlo simulations in which 32 model point sources are placed in the CLEAN-ed image and then the image is stacked at the positions of those model sources (Ikarashi et al., in preparation).

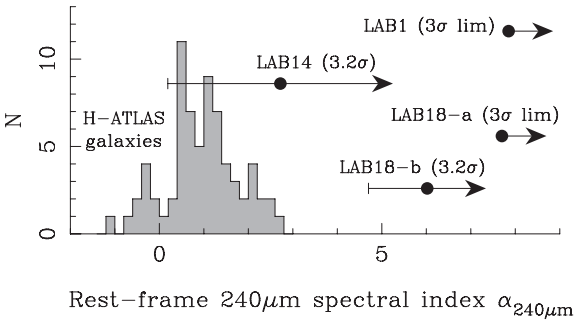

Figure 2. Constraint on the rest-frame 240-μm spectral indices of LABs at $z = 3.1$. The histogram shows $\alpha_{240\,\mu\mathrm{m}}$ found in 70 low-z *Herschel*-ATLAS SDP sources with spectroscopic redshift of $z = 0.20$–0.30, at which the *Herschel*/SPIRE 250- and 350-μm bands observe the ≈240-μm part of SEDs in the rest frame. The spectral index of LAB14 is consistent with those of H-ATLAS galaxies. However, indices of LAB1 and LAB18-a/b cannot be explained.

In Fig. 3 (left-hand panel), we show the results of the stacking analysis for the 32 LABs; the mm emission is not statistically detected. The weighted mean of the 1.1-mm flux density constrains the typical 1.1-mm flux density, and thus the L_{FIR} for LABs. We put the 3σ upper limit of $S_{1.1\,\mathrm{mm}} < 0.40$ mJy, which corresponds to $L_{\mathrm{FIR}} < 4.5 \times 10^{11}\,\mathrm{L}_\odot$ and $M_{\mathrm{dust}} < 1 \times 10^8\,\mathrm{M}_\odot$ if assuming $T_{\mathrm{dust}} = 35$ K, $\beta = 1.5$ and the dust emissivity $\kappa_{\mathrm{d}}(850\,\mu\mathrm{m}) = 0.1\ \mathrm{m^2\ kg^{-1}}$ (Hildebrand 1983). As shown in Fig. 2, a realistic $\alpha_{240\,\mu\mathrm{m}}$ is likely in the range between −1 and 3, which makes the 850-to-1100-μm flux ratio of 0.8 to 2.2. The 1.1-mm 3σ upper limit thus corresponds to 0.3–0.9 mJy at 850 μm. This is below the mean 850-μm flux density of all the LABs observed by SCUBA (3.0 ± 0.9 mJy; Geach et al. 2005), but is still consistent with a mean 850-μm flux of 1.2 ± 0.4 mJy derived only for the LABs which are not individually detected at 850 μm (Geach et al. 2005). The right-hand panel of Fig. 3 shows the 1.1-mm stacked image for the SCUBA-detected LABs. The noise level is 0.44 mJy beam^{-1}. We do not significantly detect 1.1-mm emission in the SCUBA-LABs; however, we see a small 2.3σ peak. We derive a 3σ upper limit of $S_{1.1\,\mathrm{mm}} < 3.3$ mJy, yielding

[3] LAB14, 18 and 34 are masked.
[4] LAB14 and 18 are masked.

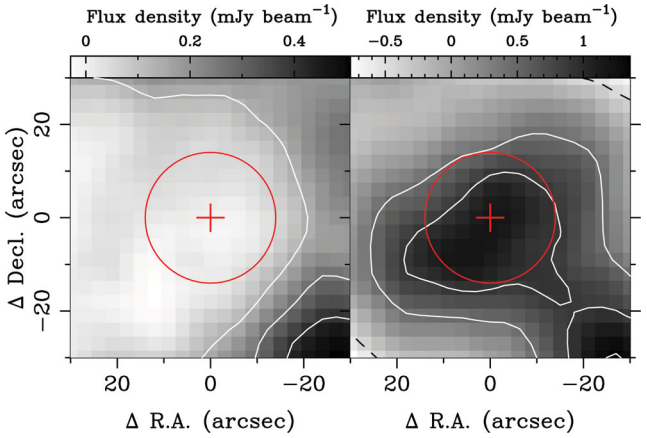

Figure 3. The 1.1-mm stacked images at the positions of 32 LABs (left) and 3 SCUBA-detected LABs (right). The 1σ noise levels at 1.1 mm are 0.135 and 0.44 mJy beam^{-1}, respectively. The contours start from 1σ with an interval of 1σ, and the negative signals are indicated by dotted contours. The red circle and cross on each panel indicate the HPBW of AzTEC/ASTE and the nominal position of LABs. No significant emission was found in both samples, although a small peak is seen (2.3σ) in the stacked image of the SCUBA-detected LABs.

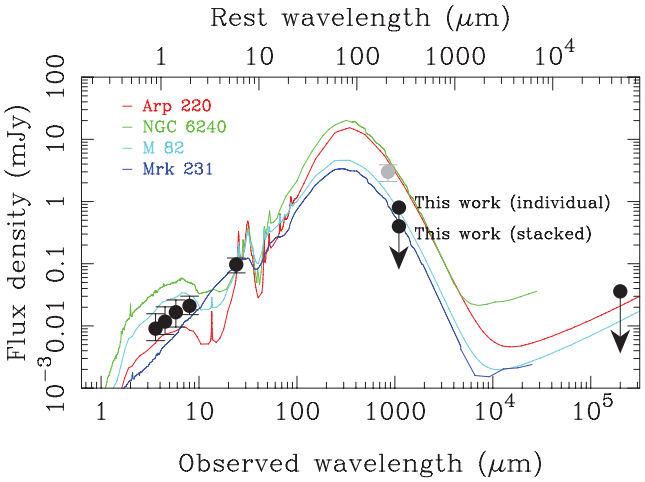

Figure 4. The composite SED of the 24-μm–detected LABs (LAB1, LAB14, LAB16 and LAB18; Webb et al. 2009). The filled circles and error bars of IRAC and MIPS photometry (3.6–24 μm) represent the mean and minimum–maximum of the flux densities of the four LABs. We also show the averaged 850-μm flux (grey circle) and a VLA 21-cm 3σ upper limit. The template SEDs are normalized by the mean 24-μm flux of these LABs.

$L_{\rm FIR} < 1.4 \times 10^{12}\,{\rm L}_\odot$ and $M_{\rm dust} < 3 \times 10^8\,{\rm M}_\odot$ if assuming $T_{\rm dust} = 35$ K, $\beta = 1.5$ and $\kappa_{\rm d}(850\,\mu{\rm m}) = 0.1$ m^2 kg^{-1}.

4 DISCUSSIONS AND CONCLUSIONS

We have conducted 1.1-mm observations with AzTEC/ASTE to map the SSA22 field, which is known for having an overdensity of $z = 3.1$ LABs, as well as LAEs. None of the individual 35 LABs have been detected at 1.1 mm, though LAB14 (and possibly LAB18 also) has a marginal signal (3.2σ). Our stacking analysis for 32 LABs fails to statistically detect the 1.1-mm emission ($S_{1.1\,{\rm mm}} < 0.40$ mJy, 3σ), suggesting that LABs on average have little ultraluminous obscured star formation ($L_{\rm FIR} < 4.5 \times 10^{11}\,{\rm L}_\odot$ [3σ], if assuming $T_{\rm dust} = 35$ K and $\beta = 1.5$), unlike a long-believed picture that many LABs undergo intense dusty star formation with SFRs of $\sim 10^3\,{\rm M}_\odot\,{\rm yr}^{-1}$ (Chapman et al. 2001, 2004; Geach et al. 2005).

We compile the results of previous mm/sub-mm observations of LABs (>30 kpc) at various redshifts (Smail et al. 2003; Greve et al. 2007; Matsuda et al. 2007; Beelen et al. 2008; Saito et al. 2008; Smith et al. 2008; Bussmann et al. 2009; Ouchi et al. 2009; Walter et al. 2012; Yang et al. 2012, and this work), and find that the detection rate of mm and sub-mm emission in individual LABs is 4/48 (8.3 per cent) (Smail et al. 2003; Greve et al. 2007; Beelen et al. 2008; Yang et al. 2012, for sub-mm–detected LABs) though the sensitivities are not uniform. This value is lower than previously suggested (5/25 = 20 per cent; Geach et al. 2005), but at least a small fraction (∼10 per cent) of LABs may undergo obscured starbursts. Although the bulk of LABs appear not to have starbursts as seen in SMGs, massive (10^{10}–$10^{11}\,{\rm M}_\odot$) stellar components are broadly seen within the Lyα haloes (Geach et al. 2007; Uchimoto et al. 2008; Smith et al. 2008; Ouchi et al. 2009).

Moreover, 4 of 26 (15 per cent) and 5 of 29 (17 per cent) of the LABs in SSA22 have 24 μm and X-ray sources, respectively (Geach et al. 2009; Webb et al. 2009), suggesting that 15–20 per cent of LABs may host obscured star formation and/or AGN activities, regardless of whether they are detected at 1.1 mm. Fig. 4 shows the composite mid-IR to radio SED of the 24-μm-detected LABs (LAB1, LAB14, LAB16 and LAB18-a; Webb et al. 2009). Two of them (LAB14 and LAB18) are detected in the X-rays (Geach et al. 2009). We also show SEDs of local starburst galaxies Arp 220, NGC 6240, M82 (Silva et al. 1998) and a nearby IR-luminous quasar Mrk 231 (Berta 2005). The FIR luminosities of Arp 220, NGC 6240, M82 and Mrk 231 are $L_{\rm FIR} = 1.4 \times 10^{12}$, 5.4×10^{11}, $4.1 \times 10^{10}\,{\rm L}_\odot$ and $2.0 \times 10^{12}\,{\rm L}_\odot$ (Sanders et al. 2003), respectively. The template SEDs are redshifted to $z = 3.09$ and normalized by the mean 24-μm flux of the four LABs. M82 and Mrk 231 have warmer dust than Arp 220 and NGC 6240, and this is why the (sub-)mm fluxes of the M82 and Mrk 231 templates are lower than the others. The 1.1-mm upper limits are better consistent with the extrapolation of the M82 and Mrk 231 SEDs than Arp 220 and NGC6240. This suggests that the 24-μm objects within the four LABs are powered by star formation and/or AGN activities that are enough to maintain the dust temperatures high, but lack a large reservoir of cooler gas and dust which is often seen in SMGs ($M_{\rm dust} \sim 10^9\,{\rm M}_\odot$, e.g. Kovács et al. 2006; Michałowski, Hjorth & Watson 2010).

These evidences may imply that some LABs are at a phase where the extreme starburst phase has just been quenched for some reason, for example, by dissociation of molecular clouds by a superwind from a nuclear starburst and/or AGN. On the other hand, ∼30 per cent of LABs do not host any bright UV continuum sources in the halo (e.g. Matsuda et al. 2004; Nilsson et al. 2006); such LABs without UV continuum sources may result from cooling radiation of cold streams as suggested by many authors (e.g. Nilsson et al. 2006).

Although the non-detections reported here put a constraint on the obscured SFR of the LABs, they do not rule out any possibilities for the formation mechanisms of Lyα nebulosity. If all of the Lyα emission observed in the LABs is attributed to ionizing photons from young massive stars, the Lyα luminosities correspond to SFRs of ≈10–100 $\,{\rm M}_\odot\,{\rm yr}^{-1}$ following the expression $L_{{\rm Ly}\alpha} = 1.0 \times 10^{42}\,({\rm SFR}/{\rm M}_\odot\,{\rm yr}^{-1})$ erg s^{-1} (Osterbrock & Ferland 1989; Kennicutt 1998). Our constraint on the FIR luminosity ($L_{\rm FIR} < 4.5 \times 10^{11}\,{\rm L}_\odot$) suggests that SFR obscured by dust is less than $80\,{\rm M}_\odot\,{\rm yr}^{-1}$, following Kennicutt (1998). This limit is comparable to the Lyα-derived SFR, but is not small enough to fully rule out the

possibility that the Lyα nebulosity is produced by feedback from massive star formation activity. Smith et al. (2008) claimed that their non-detection of 1.2-mm emission in a $z = 2.8$ LAB ($L_{\mathrm{Ly}\alpha} = 2.1 \times 10^{43}$ erg s^{-1}), which limits the SFR to <220 M$_\odot$ yr^{-1} (assuming $T_{\mathrm{dust}} = 35$ K and $\beta = 1.5$), rules out the photoionization scenario in favour of the cold accretion scenario. We consider, however, that the interpretation still leaves room for reconsideration, since only an SFR of 21 M$_\odot$ yr^{-1} is able to produce the Lyα luminosity of the $z = 2.8$ LAB and so the SFR limit (<220 M$_\odot$ yr^{-1}) from the 1.2-mm measurement is not enough to exclude the photoionization scenario.

Obviously, one of the reasons why the formation mechanism of LABs is so ambiguous is that we do not have a complete picture of obscured star formation activity within LABs. The sensitivity of the AzTEC/ASTE imaging survey presented in this work is confusion limited, and higher resolution imaging with higher sensitivity such as possible with ALMA is needed to give a better understanding of the formation mechanism of LABs.

ACKNOWLEDGEMENTS

We would like to acknowledge the AzTEC/ASTE team who made the observations possible. We thank T. Yamada and T. Hayashino for providing the Subaru images. We would also like to thank R. Ivison for providing the new VLA image. YT is supported by JSPS Grant-in-Aid for Research Activity Start-up (no. 23840007). KSS is supported by the National Radio Astronomy Observatory, which is a facility of the National Science Foundation operated under cooperative agreement by Associated Universities, Inc. BH is supported by Research Fellowship for Young Scientists from JSPS. AzTEC/ASTE observations were partly supported by KAKENHI (no. 19403005, 20001003). The ASTE project is driven by Nobeyama Radio Observatory (NRO), a branch of NAOJ, in collaboration with University of Chile, and Japanese institutes including University of Tokyo, Nagoya University, Osaka Prefecture University, Ibaraki University and Hokkaido University. The *Herschel*-ATLAS is a project with *Herschel*, which is an ESA space observatory with science instruments provided by European-led principal investigator consortia and with important participation from NASA. The H-ATLAS website is http://www.h-atlas.org/.

REFERENCES

Beelen A. et al., 2008, A&A, 485, 645
Berta S., 2005, PhD thesis, Padova University
Blain A. W., Smail I., Ivison R. J., Kneib J.-P., Frayer D. T., 2002, Phys. Rep., 369, 111
Bussmann R. S. et al., 2009, ApJ, 705, 184
Chapman S. C., Lewis G. F., Scott D., Richards E., Borys C., Steidel C. C., Adelberger K. L., Shapley A. E., 2001, ApJ, 548, L17
Chapman S. C., Scott D., Windhorst R. A., Frayer D. T., Borys C., Lewis G. F., Ivison R. J., 2004, ApJ, 606, 85
Chapman S. C., Blain A. W., Smail I., Ivison R. J., 2005, ApJ, 622, 772
Colbert J. W., Scarlata C., Teplitz H., Francis P., Palunas P., Williger G. M., Woodgate B., 2011, ApJ, 728, 59
Downes T. P., Welch D., Scott K. S., Austermann J., Wilson G. W., Yun M. S., 2012, MNRAS, 423, 529
Eales S. et al., 2010, PASP, 122, 499
Ezawa H., Kawabe R., Kohno K., Yamamoto S., 2004, Proc. SPIE, 5489, 763
Fardal M. A., Katz N., Gardner J. P., Hernquist L., Weinberg D. H., Davé R., 2001, ApJ, 562, 605
Geach J. E. et al., 2005, MNRAS, 363, 1398
Geach J. E., Smail I., Chapman S. C., Alexander D. M., Blain A. W., Stott J. P., Ivison R. J., 2007, ApJ, 655, L9
Geach J. E. et al., 2009, ApJ, 700, 1
Greve T. R., Stern D., Ivison R. J., De Breuck C., Kovács A., Bertoldi F., 2007, MNRAS, 382, 48
Hayashino T. et al., 2004, AJ, 128, 2073
Hildebrand R. H., 1983, QJRAS, 24, 267
Högbom J. A., 1974, A&AS, 15, 417
Holland W. S. et al., 1999, MNRAS, 303, 659
Kennicutt R. C., Jr, 1998, ARA&A, 36, 189
Kovács A., Chapman S. C., Dowell C. D., Blain A. W., Ivison R. J., Smail I., Phillips T. G., 2006, ApJ, 650, 592
Matsuda Y. et al., 2004, AJ, 128, 569
Matsuda Y., Yamada T., Hayashino T., Yamauchi R., Nakamura Y., 2006, ApJ, 640, L123
Matsuda Y., Iono D., Ohta K., Yamada T., Kawabe R., Hayashino T., Peck A. B., Petitpas G. R., 2007, ApJ, 667, 667
Matsuda Y. et al., 2011, MNRAS, 410, L13
Michałowski M., Hjorth J., Watson D., 2010, A&A, 514, A67
Mori M., Umemura M., 2006, Nat, 440, 644
Nilsson K. K., Fynbo J. P. U., Møller P., Sommer-Larsen J., Ledoux C., 2006, A&A, 452, L23
Ohyama Y. et al., 2003, ApJ, 591, L9
Osterbrock D. E., Ferland G. J., 1989, Astrophysics of Gaseous Nebulae and Active Galactic Nuclei. University Science Books, Mill Valley, CA
Ouchi M. et al., 2009, ApJ, 696, 1164
Pascale E. et al., 2011, MNRAS, 415, 911
Rigby E. E. et al., 2011, MNRAS, 415, 2336
Saito T., Shimasaku K., Okamura S., Ouchi M., Akiyama M., Yoshida M., 2006, ApJ, 648, 54
Saito T., Shimasaku K., Okamura S., Ouchi M., Akiyama M., Yoshida M., Ueda Y., 2008, ApJ, 675, 1076
Sanders D. B., Mazzarella J. M., Kim D.-C., Surace J. A., Soifer B. T., 2003, AJ, 126, 1607
Scott K. S. et al., 2008, MNRAS, 385, 2225
Silva L., Granato G. L., Bressan A., Danese L., 1998, ApJ, 509, 103
Smail I., Ivison R. J., Gilbank D. G., Dunlop J. S., Keel W. C., Motohara K., Stevens J. A., 2003, ApJ, 583, 551
Smith D. J. B., Jarvis M. J., Lacy M., Martínez-Sansigre A., 2008, MNRAS, 389, 799
Smith D. J. B. et al., 2011, MNRAS, 416, 857
Steidel C. C., Adelberger K. L., Shapley A. E., Pettini M., Dickinson M., Giavalisco M., 2000, ApJ, 532, 170
Tamura Y. et al., 2009, Nat, 459, 61
Tamura Y. et al., 2010, ApJ, 724, 1270
Taniguchi Y., Shioya Y., 2000, ApJ, 532, L13
Taniguchi Y., Shioya Y., Kakazu Y., 2001, ApJ, 562, L15
Uchimoto Y. K. et al., 2008, PASJ, 60, 683
Walter F. et al., 2012, ApJ, 752, 93
Webb T. M. A., Yamada T., Huang J.-S., Ashby M. L. N., Matsuda Y., Egami E., Gonzalez M., Hayashimo T., 2009, ApJ, 692, 1561
Wilson G. W. et al., 2008, MNRAS, 386, 807
Yang Y. et al., 2012, ApJ, 744, 178

This paper has been typeset from a TEX/LATEX file prepared by the author.